Numerical Simulations of NBI-driven GAE modes in L-mode and H-mode Discharges in NSTX

E. V. Belova[1], N. N. Gorelenkov[1], E. D. Fredrickson[1], H. L. Berk[2], G. J. Kramer[1], S. S. Medley[1]

[1] Princeton Plasma Physics Laboratory, Princeton NJ, USA

[2]University of Texas, Austin TX, USA

E-mail contact of main author: ebelova@pppl.gov

Abstract. Hybrid 3D code HYM has been used to investigate properties of beam ion driven GAE modes in NSTX. The HYM code is a nonlinear, global stability code in toroidal geometry, which includes fully kinetic ion description. Excitation of GAE modes have been studied for L-mode and H-mode NSTX discharges. Equilibrium profiles and plasma parameters have been chosen to match several of the NSTX discharge numbers profiles, and the HYM equilibrium solver has been modified to improve the equilibrium fit to the TRANSP and EFIT profiles. Numerical simulations for H-mode have been performed for the NSTX shots, where a GAE activity and related High-Energy Feature (HEF) have been observed. HYM simulations comparison with experimental results for NSTX L-mode shots, show good agreement in terms of the most unstable toroidal mode numbers, frequency, amplitude and the mode structure. It has been shown that most resonant particles have stagnant orbits, and poloidal structure of the unstable mode is relatively coincident with location of the resonant orbits. Linearized and nonlinear simulations have been performed in order to study in detail resonant wave-particle interaction in order to understand the nonlinear evolution of the instability.

1. Introduction

Experimental observations from NSTX suggest that many modes in a sub-cyclotron frequency range are excited during neutral beam injection (NBI). As was shown recently, these modes can induce strong anomalous electron transport [1], and it is suggested that these modes can cause a redistribution of fast ions [2,3]. Sub-cyclotron frequency modes were identified as Compressional Alfven Eigenmodes (CAEs) and Global Alfven Eigenmodes (GAEs), driven unstable through the Doppler shifted cyclotron resonance with the super Alfvenic NBI ions. These modes can be excited in ITER due to super Alfvenic velocities and strong anisotropy of the beam ions. In addition, the high frequency modes can also be excited by alpha particles near the outer edge of ITER plasma due to anisotropies in alpha particle distribution, and could be used as a diagnostic for ITER alphas. Hybrid 3D code HYM [5] has been used to investigate properties of beam ion driven GAE modes in NSTX. The HYM code is a nonlinear, global stability code in toroidal geometry, which includes fully kinetic ion description. A generalized form of the Grad-Shafranov equation solver has been developed, which includes, non-perturbatively, the effects of the beam ions with anisotropic distribution [6]. Excitation of GAE modes have been studied for L-mode and H-mode NSTX discharges. Equilibrium profiles and plasma parameters have been chosen to match several of the NSTX discharge numbers profiles, using the TRANSP and EFIT codes.

2. Simulations of L-mode discharge

2.1. Comparison with experimental results

HYM simulations comparison with experimental results for NSTX L-mode shot#135419 [3], show good agreement in terms of the most unstable toroidal mode numbers, mode frequency, and mode structure. Several modes are found to be unstable with toroidal mode numbers n=6 - 9 and frequencies f=0.4-0.8MHz (plasma frame) compared to experimental results of n=7 - 11, and f=0.8-1MHz. In the simulations, these modes have been identified as counter-rotating GAE modes based on large perpendicular component of perturbed magnetic field in the core, however large compressional component has been found at the edge for all unstable GAE modes. Time evolution of magnetic field perturbation and density perturbation for the n=9 mode are shown in Fig. 1. For the n=9 GAE mode, mode frequency f =1.02MHz, amplitude $\delta n/n \approx 0.2\%$, and linear growth rate $\gamma/\omega=3.4\%$ compare with measured mode frequency f≈950 kHz, amplitude $\delta n/n \approx 0.1\%$, and estimated growth rate [3,4]. The magnetic perturbations have shear Alfven wave polarization in the core with dominant $\delta B_\perp$ (Fig. 1b), however they also have significant compressional component with $\delta B_\parallel \sim 1/3 \cdot \delta B_\perp$. Strong coupling between shear Alfven waves and compressional perturbations in the NSTX simulations is related to small aspect-ratio and kinetic effects due to energetic particles. The compressional component is found to be larger than perpendicular component of $\delta\mathbf{B}$ at the edge (Fig.1a), which is also observed in magnetic measurements in NSTX [3]. Radial mode structure of the n=9 GAE mode has been found to be consistent with the inferred perpendicular displacement profile for this mode [4].

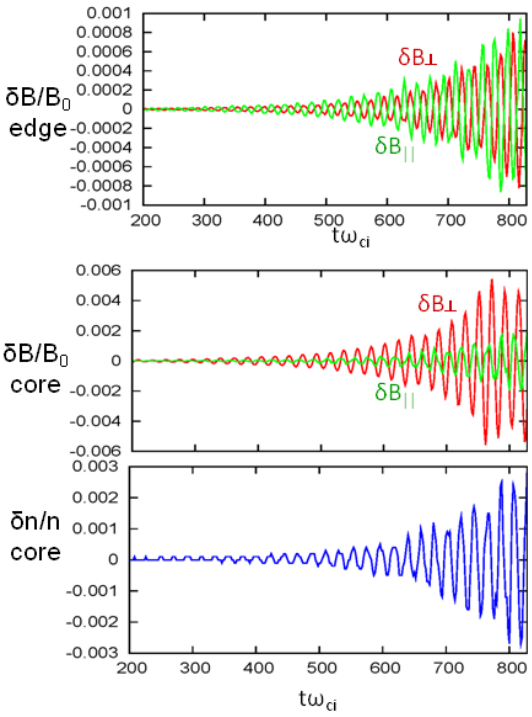

FIG. 1. *Time evolution of perpendicular and parallel components of magnetic field perturbation and density perturbation from HYM simulations for NSTX shot #135419, GAE mode with* $\omega=0.29\omega_{ci0}$, $\gamma=0.01\omega_{ci0}$, *(n=9, m=-1).*

2.2. Analysis of resonant wave-particle interaction

Linearized and nonlinear simulations have been performed in order to study in detail resonant wave-particle interaction (Fig. 2). The resonant particles are shown to satisfy Doppler-shifted cyclotron resonant conditions, and multiple resonances are found for each toroidal mode number (Fig. 2b). General resonant condition can be written as: $\omega - l\langle\omega_{ci}\rangle - \langle k_{||}v_{||}\rangle - \langle k_\perp v_D\rangle = 0$, where brackets denote orbit averaging, and $\omega_{ci} \sim B_0(1+\varepsilon\cos\theta)$, $k_\perp v_D \sim \sin(\psi+\theta)$ are cyclotron frequency and perpendicular drift frequency along the particle orbit. After orbit averaging, the resonant condition becomes: $\omega - l\langle\omega_{ci}\rangle - (nq-m)\langle v_{||}/qR\rangle - (p+r)\langle v_{||}/qR\rangle = 0$, where p and r are arbitrary integers. Therefore, for each poloidal mode number m there will be multiple resonances corresponding to $m' = m - (p + r)$. Alternatively, for each particle (passing or trapped), three frequencies associated with particle equilibrium motion can be calculated: $\langle\omega_{ci}\rangle$, ω_{tor}, and ω_{pol}, corresponding to particle periodic motion in magnetic field, toroidal

direction, and poloidal plane. In this case, the most general form of the resonant condition becomes: $\omega - l\langle\omega_{ci}\rangle + n\omega_{prec} + k\omega_{transit} = 0$, where ω_{prec} and $\omega_{transit}$ correspond to orbit-averaged ω_{tor}, and ω_{pol} , respectively. This diagnostic has been implemented in the HYM code.

The energetic particle model in the HYM code uses the delta-f scheme, where perturbed part of the distribution function is evolved along the particle orbit. This allows to sort simulation particles into resonant and non-resonant, based on the relative values of their weight which is proportional to the change in the distribution function $w \sim \delta F$. It is assumed that the resonant particles will have a large relative change in the value of $\delta F/F$. Location of the resonant particles in the phase-space and the resonant condition have been examined in the simulations of the n=9 GAE mode. Figure 2a shows location of the resonant particles in the λ-ε space, there two distinct groups of resonant particles can be seen, but with similar values of $v_{\|}$ ($\lambda = \mu B_0/\varepsilon$ is a pitch angle parameter, and $\varepsilon = mv^2/2$ is particle energy). Particle colours correspond to different energies: from E=0 (purple) to E=80keV (red). It is seen that resonant particles occupy a wide range of energies. Figure 2b shows that resonant particles satisfy condition: $\omega - \langle\omega_{ci}\rangle + n\omega_{prec} + k\omega_{transit} = 0$, where n=9, and k=0,±1,±2,… Transit (poloidal) frequency is small compared to other terms in the resonant condition, with $\omega_{transit}$=0.06-0.08 ω_{ci0}, resulting in the fine splitting of resonances in Fig. 2b, where the solid green line corresponds to condition $\langle\omega_{ci}\rangle = \omega + n\cdot\omega_{prec}$. The spread in the values of $\omega_{transit}$ is comparable to the mode growth rate, γ=0.01 ω_{ci0}.

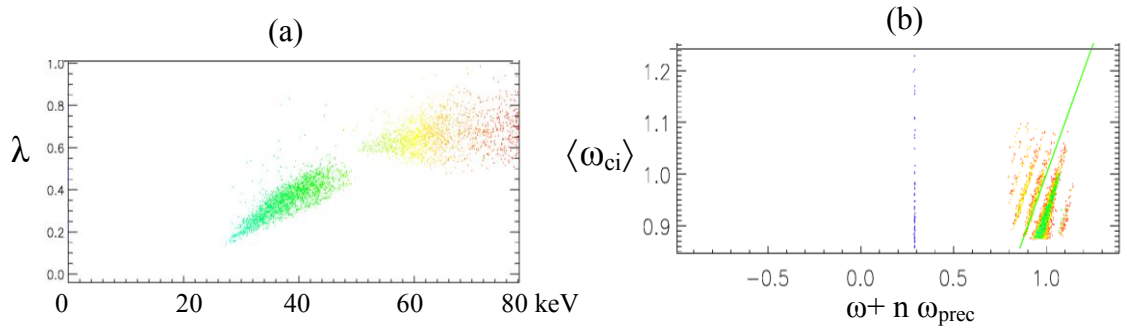

FIG. 2. *(a) Location of resonant particles in phase space, $\lambda=\mu B_0/\varepsilon$ vs energy, (b) resonant particles shown with orbit-averaged cyclotron and precession frequencies, both normalized to the ion cyclotron frequency at the axis, ω_{ci0}. From HYM simulations for NSTX shot #135419, $\omega=0.29\omega_{ci0}$, $\gamma=0.01\omega_{ci0}$, (n=9, m=-1). Particle colour corresponds to different energies: from E=0 (purple) to E=80keV (red).*

The delta-f model implemented in the HYM code, also allows detailed analysis of the instability drive, since time advance of the particle weights includes calculation of the terms in the derivative of the distribution function. That is

$$\frac{d}{dt}\delta f = -\frac{d}{dt} f_0 = -\frac{d\varepsilon}{dt}\frac{\partial f_0}{\partial \varepsilon} - \frac{dp_\phi}{dt}\frac{\partial f_0}{\partial p_\phi} - \frac{d\lambda}{dt}\frac{\partial f_0}{\partial \lambda}$$

where the three terms on the right-hand-side correspond to dependence of the equilibrium distribution function on particle energy, toroidal angular momentum, and the pitch-angle parameter. By turning off different terms in the equation for the particle weights, it has been demonstrated that first two terms have stabilizing effect on the instability, whereas distribution function anisotropy related to the dependence on the pitch angle parameter is

responsible for the instability drive. In the HYM code, the pitch-angle parameter dependence is assumed to be in the form $F(\lambda) \sim \exp((\lambda-\lambda_0)^2/\Delta\lambda^2)$, where $\lambda_0=0.7$, $\Delta\lambda=0.36$, and with slowing-down and power dependence on energy and toroidal momentum, respectively [6].

Analysis of the particle orbits and mode structure for these simulations has shown that most resonant particles have near-stagnant orbits, and there is relatively small variation of the background magnetic field along the orbit. Poloidal structure of the unstable mode is found to be relatively coincident with location of the resonant orbits, thus allowing for a strong resonant interaction. Nonlinear simulations show that GAE instabilities saturate at low amplitudes due to particle trapping, with saturation amplitude being proportional to the square of the linear growth rate.

3. GAE mode structure in H-mode simulations

3.1. NSTX shot #132800

Numerical simulations have been performed for H-mode, NSTX shot #132800 (with I_p = 1.0 MA, B_T = 4.5 kG, E_B = 90 keV), where a robust GAE activity and related High-Energy Feature (HEF) have been observed [2]. Figure 3a shows comparison between EFIT and HYM equilibrium poloidal flux contours and toroidal magnetic field contours. It has been found that self-consistent equilibrium with anisotropic fast ion distribution has larger magnetic axis radius compared to the MHD equilibrium solution from TRANSP (Fig. 3a). Simulations show unstable GAE for n ~ 6 – 9, consistent with Mirnov coil data. The n=7, m=-1 GAE mode exhibits the largest growth rate with $\gamma=0.02\omega_{ci0}$ and $\omega=0.21\omega_{ci0}$ (f=600kHz), the n=6 and n=8 are also unstable with smaller growth rates. Figures 3b and 3c show contour plots of plasma pressure perturbation in poloidal plane for n=7 and n=6 GAE modes.

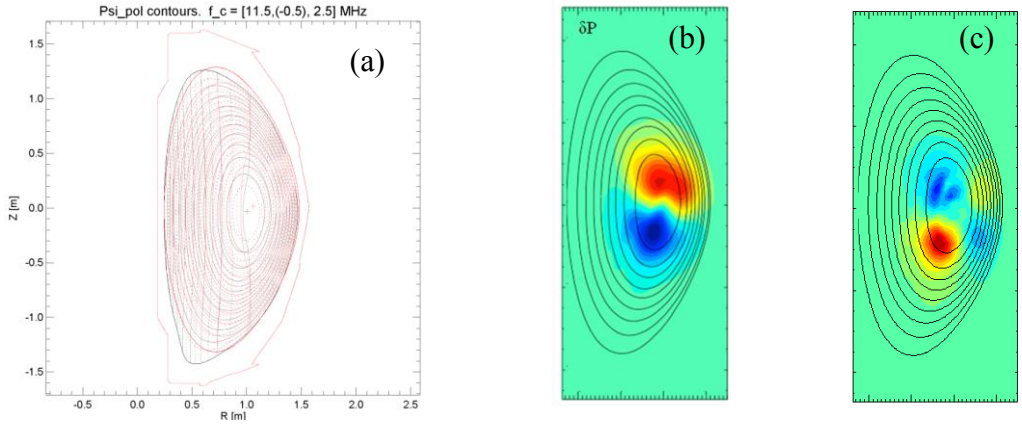

FIG. 3. (a) Comparison between EFIT and HYM equilibrium poloidal flux contours and toroidal magnetic field contours; (b) pressure perturbation for n=7,m=-1 and (c) n=6, m=-2 GAE modes from simulations of NSTX shot #132800.

3.2. NSTX shot #141398

Detailed measurements of GAE and CAE modes amplitudes and mode structure were obtained for H-mode plasma in NSTX shot 141398 [7]. These measurements show mode structure from the plasma edge to the core, and can be used for comparison with numerical simulation results, and code validation. The modes have been identified as CAE modes for frequencies f>600 kHz, and small toroidal mode numbers |n|≤5, and as GAEs for f<600 kHz, and |n|~6-8 based on dispersion relations [7].

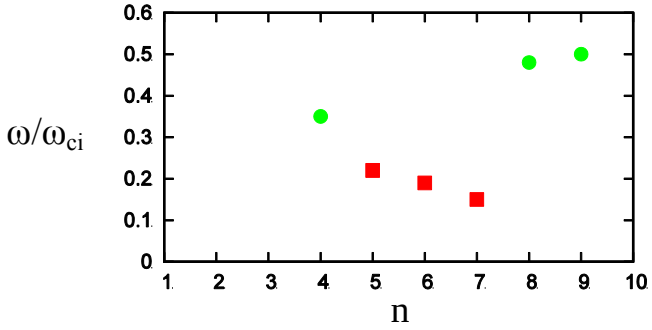

FIG. 4. Mode frequency versus toroidal mode number for most unstable GAE (red) and CAE (green) modes, from HYM simulations for NSTX shot #141398. Frequency is normalized to the ion cyclotron frequency at the axis f_{ci}=2.5MHz.

HYM linearized simulations for this shot show that most unstable modes for n=5-7 are counter-rotating GAE modes, which have shear Alfven wave polarization in the core, and comparable parallel and perpendicular components of perturbed magnetic field at the edge. The n=4 and n=8 and 9 modes are co-rotating CAE modes, which have been identified based on large compressional component of perturbed magnetic field both at the edge and in the core. Figure 4 shows mode frequency versus toroidal mode number for both GAE and CAE modes. All unstable modes have small poloidal mode numbers with m≤3. Measured growth rates for n=5-7 modes are γ/ω_{ci}= 0.014, 0.035, and 0.035 respectively, whereas the linear growth rates for CAEs are significantly smaller with γ/ω_{ci}= 0.005, 0.004, and 0.0014 for the n=4, 8, and 9 modes respectively.

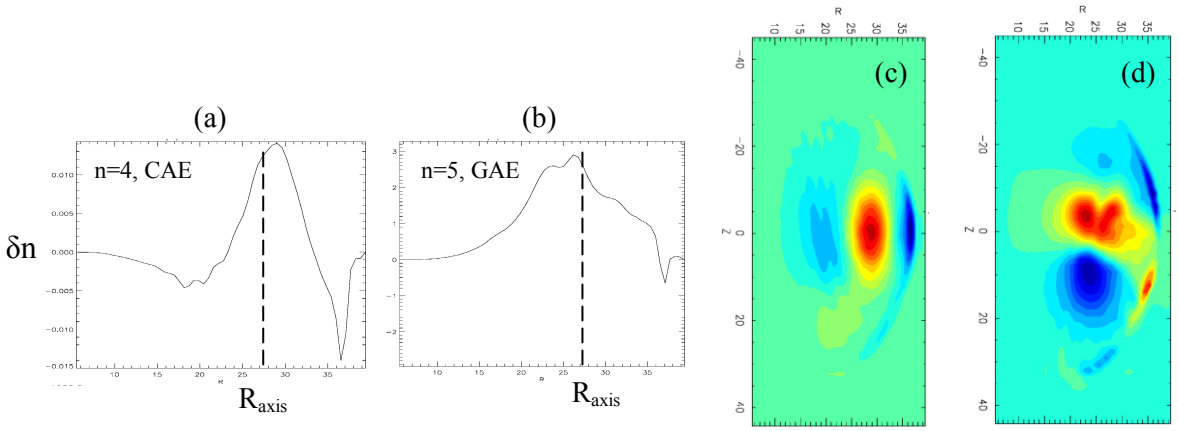

FIG.5. (a-b) Radial profiles of density perturbation for the n=4 CAE mode and the n=5 GAE mode versus major radius; (c-d) contour plots of density perturbation for the n=4 CAE and the n=5 GAE modes. Magnetic axis location is shown by dashed line.

Figure 5 shows density perturbation radial profiles and poloidal contour plots for the n=4 CAE ($\omega=0.35\omega_{ci}$) and n=5 GAE ($\omega=0.22\omega_{ci}$) modes. R is major radius in code units (1 unit=3.93cm), and the magnetic axis is located approximately at R=27.5 and plasma edge is at R~37.5. It can be seen that the GAE mode has wider radial profile, and the CAE mode has more narrow radial structure, which is consistent with larger frequency for smaller n and m values compared to the n=5 mode. Another major difference between CAE and GAE modes is that for CAEs, $\delta B_{\|}$ is significantly larger than $\delta B_{\perp}$ everywhere including the edge, whereas for GAEs, $\delta B_{\|}$ is comparable to $\delta B_{\perp}$ only at the edge.

Resonant particle plots for the n=8 co-rotating CAE mode (Fig.6) show two separate groups of the resonant particles, one group which satisfy the regular resonance condition: $\omega - k_{||}v_{||} = 0$, and another which satisfy the Doppler-shifted cyclotron resonant condition: $|\omega| + \omega_{ci} - k_{||}v_{||} = 0$. In contrast to the resonant condition for the GAE modes, the Doppler shift is larger than the orbit-averaged cyclotron frequency for the large-n CAE modes.

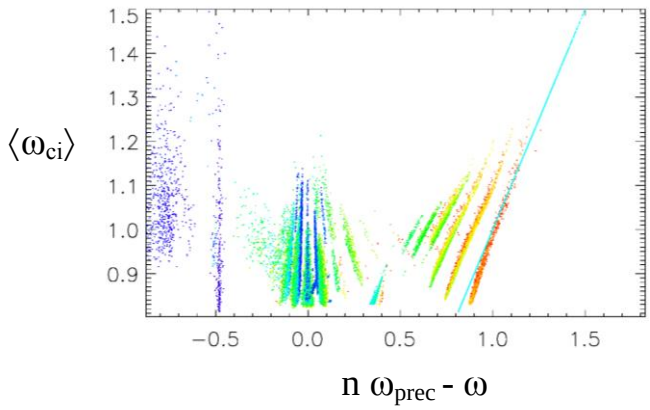

FIG. 6. Scatter plot showing orbit-averaged cyclotron and precession frequencies of resonant particles (normalized to the ion cyclotron frequency at the axis, ω_{ci0}). From HYM simulations for NSTX shot #141398 of the n=8 co-rotating CAE mode with $\omega=0.48\omega_{ci}$. Particle colour corresponds to different energies: from E=0 (purple) to E=80keV (red).

Unstable CAE modes have not been observed in the previous L-mode simulations. Conditions favorable for the excitation of these modes are been investigated. The HYM code is the initial-value code, therefore only the most unstable modes can be observed in the linear simulations for a given toroidal mode number. However the calculated range of the unstable toroidal mode numbers, frequencies, and mode polarizations appear to be reasonably close to the experimentally observed parameters [7]. More detailed comparisons of the mode frequencies and structure with the experimental data will be performed in the future.

4. Conclusion

Self-consistent 3D hybrid MHD/kinetic simulations have been performed to study the excitation of sub-cyclotron frequency Alfven eigenmodes in the NSTX. Simulations consistently show unstable GAE modes in both L-mode and H-mode discharges, and co-rotating CAE modes have been found unstable in the H-mode simulations. Self-consistent mode structure obtained in these simulations can be used to compare with experimental measurements, and to study the effects of these modes on the energetic particles distribution (HEF) or on the electron transport using test-particle codes.

Recent experimental observations from NSTX suggest that modes in a sub-cyclotron frequency range can induce strong anomalous electron transport in STs[1]. In order to study the effects of these modes on the electron transport, a kinetic description for the electrons has been implemented in the HYM code, where the electrons are described as delta-f drift-kinetic particles. Future plans include the study of the effects of GAE and CAE modes on the electron transport using both test particle and self-consistent simulations.

5. Acknowledgements

The simulations reported here were carried out using resources of the National Energy Research Scientific Computing Center (NERSC). This research was supported by the U.S. Department of Energy.

[1] D. Stutman, et al., "Correlation between Electron transport and Shear Alfven Activity in the National Spherical Torus Experiment", Phys. Rev. Lett. **102**, 115002 (2009).

[2] S. S. Medley, et al. "Investigation of a transient energetic charge exchange flux enhancement ('spike-on-tail') observed in neutral-beam-heated H-mode discharges in the National Spherical Torus Experiment", Nucl. Fusion **52**, 013014 (2012).

[3] E. Fredrickson et al, "Observation of global Alfvén eigenmode avalanche events on the National Spherical Torus Experiment", Nucl. Fusion **52**, 043001 (2012).

[4] E. Fredrickson et al., "Observation of Global Alfven Eigenmode Avalanche events on the National Spherical Torus Experiment", Proc. of 23rd IAEA FEC, Daejon, Korea, October 2010, EXW/P7-06 (2010).

[5] E. V. Belova, et al., "Numerical study of tilt stability of prolate field-reversed configurations", Phys. Plasmas **7**, 4996 (2000).

[6] E.V. Belova, N.N. Gorelenkov, C.Z. Cheng, "Self-consistent equilibrium model of low aspect-ratio toroidal plasma with energetic beam ions", Phys. Plasmas, **10**, 3240 (2003).

[7] N.A. Crocker, et al. "Internal Amplitude, Structure and Identification of CAEs and GAEs in NSTX", Proc. of 24th IAEA FEC, San Diego, USA, October 2012, paper EX/P6-02.